

# **CNWRA** A center of excellence in earth sciences and engineering

A Division of Southwest Research Institute™

6220 Culebra Road • San Antonio, Texas, U.S.A. 78228-5166  
(210) 522-5160 • Fax (210) 522-5155

January 4, 2002  
Contract No. NRC-02-97-009  
Account No. 20.01402.571

U.S. Nuclear Regulatory Commission  
ATTN: Mrs. Deborah A. DeMarco  
Two White Flint North  
11545 Rockville Pike  
Mail Stop T8 A23  
Washington, DC 20555

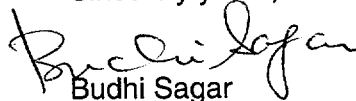
Subject: Programmatic review of Journal of Non-Crystalline Solids paper titled "Degradation of High-Level Waste Glass under Simulated Repository Conditions"

Dear Mrs. DeMarco:

Attached is the subject paper which will be submitted for publication to the Journal of Non-Crystalline Solids. The paper describes the results of leaching experiments and performance assessment calculations conducted to evaluate the effect of corrosion products on degradation of glass waste form and subsequent release of radionuclides to the environment. The paper is based on the information presented in IM 01402.571.180 titled Effect of In-Package Chemistry on the Degradation of Vitrified High-Level Radioactive Waste and Spent Nuclear Fuel Cladding which has been approved by the NRC.

Please contact Yi-Ming Pan at (210) 522-6640 if you have any questions regarding this paper.

Sincerely yours,

  
Budhi Sagar  
Technical Director

BS:YMP:jg

Enclosure

cc:	J. Linehan	J. Piccone	T. McCartin	T. Essig	Y.-M. Pan
	B. Meehan	K. Stablein	T. Ahn	W. Patrick	O. Pensado
	E. Whitt	B. Leslie	W. Reamer	CNWRA Dirs.	P. Maldonado
	J. Greeves	S. Wastler	J. Andersen	CNWRA EMs	T. Nagy (contracts)
	D. Brooks	J. Thomas	A. Henry	G. Cragolino	



Washington Office • Twinbrook Metro Plaza #210  
12300 Twinbrook Parkway • Rockville, Maryland 20852-1606

# Degradation of high-level waste glass under simulated repository conditions

Yi-Ming Pan\*, Vijay Jain, and Osvaldo Pensado

Center for Nuclear Waste Regulatory Analyses (CNWRA)  
Southwest Research Institute  
6220 Culebra Road, San Antonio, TX 78238, USA

---

## Abstract

The internal waste package environment that contains corrosion products may have a significant influence on waste form degradation. Leaching experiments of two simulated high-level waste glasses (WVDP Ref. 6 and DWPF Blend 1) were carried out in aqueous solutions of  $\text{FeCl}_2$  and  $\text{FeCl}_3$  at temperatures of 40, 70, and 90 °C that simulate the aqueous environment inside the breached waste packages. Both solution pH and the presence of corrosion species such as iron chloride were found to be major contributing factors to the net glass durability. Model abstraction and performance assessment analyses using rate expressions showed that the presence of corrosion products enhances glass dissolution and increases the subsequent release of radionuclides to the environment.

PACS: 07.05.T; 28.41.K; 61.43.F; 82.20

---

\* Corresponding author. Tel: 210-522-6640; Fax: 210-522-5184; E-mail address: [ypan@swri.org](mailto:ypan@swri.org).

## 1. Introduction

In spite of a small radionuclide inventory of high-level waste glass in the proposed high-level nuclear waste repository at Yucca Mountain, Nevada, its contribution to repository performance could be important if the radionuclide release rate from high-level waste glass is significant. The high-level waste glass corrosion process involves contact of a reactant (i.e., groundwater or water vapor) with the glass surface, chemical reaction between the reactants and glass surface, and transport of reaction products away from the reaction zone. The dissolution rate is controlled by the combination of these three processes and depends on factors such as chemical composition of the glass and solubilities of the reaction products, exposed surface area, temperature, pH, relative humidity, and chemical composition of the aqueous environment. Saturated zone groundwaters that lie below the proposed repository site are potential pathways of radionuclide transport away from the drift following waste package failure. Samples of saturated zone water pumped from J-13 Well have been used as a reference groundwater for materials testing purposes. Enrichment of chloride from evaporation experiments of synthetic J-13 Well water has been characterized to be responsible for the initial corrosion of the waste packages. As the waste packages are eventually breached, the groundwater, along with the corrosion products, will enter the inside of the waste packages. These corrosion products from the dissolution of waste package internal components may consist of iron compounds such as  $\text{FeOOH}$ ,  $\text{Fe}_2\text{O}_3$ ,  $\text{FeCl}_2$ , and  $\text{FeCl}_3$ . The chemistry of the aqueous environment inside the breached waste packages may, therefore, have a significant influence on waste form degradation.

Glass dissolution behavior has typically been investigated in aqueous conditions either with deionized water or J-13 Well water without consideration of the waste package corrosion products. However, a few studies have explored the effect of container materials and corrosion products on the glass dissolution behavior. McVay and Buckwalter[1] and Burns et al.[2] studied the effect of metals on glass dissolution behavior. While the former showed higher glass dissolution in the

presence of the ductile iron, the latter showed no significant effect on glass dissolution from 304L stainless steel, 409 and 430 ferrite steels. In addition, Burns et al.[2] showed that the A516 carbon steel had a significant detrimental effect on glass dissolution. Inagaki et al.[3], Bart et al.[4], and Werme et al.[5] studied the effect of magnetite on the glass dissolution behavior. Magnetite is considered a primary corrosion product. These studies showed that glass dissolution is enhanced by the presence of magnetite. Werme et al.[5] also studied the effect of FeOOH and concluded that glass dissolution is higher in the presence of FeOOH than in the presence of the same amount of magnetite. These studies clearly establish the effect of magnetite and FeOOH on enhancing glass dissolution.

The basic form of the rate expression adopted by U.S. Department of Energy (DOE) [6] to describe the dissolution of waste glass immersed in water is given by a form of the transition state rate law as

$$\text{Rate (g / day)} = S \left[ k_0 \cdot 10^{\eta \cdot \text{pH}} \cdot \exp\left(\frac{-E_a}{RT}\right) \cdot \left(1 - \frac{Q}{K}\right) \right] \quad (1)$$

where

$S$  — surface area of glass immersed in water, in units of  $\text{m}^2$

$k_0$  — intrinsic dissolution rate, which depends only on glass composition, in units of  $\text{g}/(\text{m}^2 \cdot \text{day})$

$\eta$  — pH dependence coefficient (dimensionless)

$E_a$  — effective activation energy, in units of  $\text{kJ/mol}$

$R$  — gas constant, which is  $8.314 \text{ J}/(\text{mol} \cdot \text{K})$

$T$  — absolute temperature in K

$Q$  — concentration of dissolved silica in the solution, in units of  $\text{g}/\text{m}^3$

$K$  — a quasi-thermodynamic fitting parameter for glass equal to the apparent silica saturation value for the glass, in units of  $\text{g}/\text{m}^3$

Equation (1) contains two main factors. The first factor is the forward rate,  $k_0 \cdot 10^{\eta \cdot \text{pH}}$   $\exp(-E_a/RT)$ , which represents the dissolution rate in the absence of concentration effects of dissolved silica (and other aqueous species involved in the backward reaction), and the other factor is the reaction affinity term  $(1 - Q/K)$ , which quantifies the effects of dissolved silica. Because of the complexity in defining parameters and associated uncertainties, a simpler bounding approach was adopted by the DOE [6] that combined  $(1 - Q/K)$  with  $k_0$ . Equation (2) was adopted as an abstraction for aqueous degradation of high-level waste glass in the Total System Performance Assessment–Site Recommendation analysis [7]:

$$\frac{\text{Rate}}{S} \text{ (g / m}^2 \cdot \text{day)} = k_{\text{eff}} \cdot 10^{\eta \cdot \text{pH}} \cdot \exp\left(\frac{-E_a}{RT}\right) \quad (2)$$

where

$$k_{\text{eff}} = k_0 \left(1 - \frac{Q}{K}\right)$$

In Eq. (2) the effective rate constant,  $k_{\text{eff}}$ , is assumed that bounds the range of the function  $k_0 (1 - Q/K)$ . This approach reduces the abstracted model to an equation involving four parameters ( $\eta$ ,  $E_a$ ,  $S$ , and  $k_{\text{eff}}$ ) and two variables (pH and  $T$ ). The model parameter values ( $k_{\text{eff}}$ ,  $\eta$ ,  $E_a$ ) in the rate expression in Eq. (2) have been determined by the DOE by regression of experimental data from single-pass flow-through and MCC-1 static leach tests for various waste glass compositions in buffer solutions prepared with deionized water [6]. However, the DOE model abstraction ignores the presence of corrosion products that could influence glass degradation.

To evaluate the effects of the internal waste package environment on degradation of high-level waste, the leaching of simulated high-level waste glasses in the presence of corrosion products was investigated. From the glass leaching results, model parameters, including the effective rate constant, pH dependence coefficient, and activation energy, were determined. An empirical rate

expression accounting for the effect of corrosion products on the glass dissolution behavior was used for performance assessment calculations to evaluate the effect of glass waste forms on radionuclide release for the proposed repository.

## 2. Experimental procedures

Two simulated high-level waste glasses, WVDP Ref. 6 and DWPF Blend 1, produced by the West Valley Demonstration Project and the Defense Waste Processing Facility, were used for dissolution studies. The environmental assessment standard reference glass, SRL EA, was tested as a baseline. The compositions of these three glasses are listed in Table 1. To simulate an internal waste package environment, deionized water containing either ferrous or ferric chlorides at concentrations of 0.0025 M and 0.25 M was used. While these test environments do not contain the ionic species present in J-13 Well water, the literature shows that dissolution of glass in deionized water is about 2 times faster than that in J-13 Well water [1]. The relatively high leach rates observed in deionized water are attributed to solution composition effects because, as elemental concentrations increase in the leachate, elemental release rates decrease. The behavior in deionized water, therefore, bounds the effects of the species present in J-13 Well water.

The test matrix is shown in Table 2. All tests were conducted using a modified product consistency test method in accordance with American Society for Testing and Materials Standard Test Method C1285 [8] except that the solutions were replaced at regular intervals. In these tests, 60-cm<sup>3</sup> perfluoroalkoxy TFE-fluorocarbon vessels were used. Approximately 3 g of crushed glass with a particle size distribution between - 100 to +200 mesh was placed in each vessel. A 30-cm<sup>3</sup> test solution was added to each vessel, giving a glass surface area to solution volume ratio of 2,000 m<sup>-1</sup>, as calculated in C1285. The vessels were placed in ovens held at a temperature of 90 °C. The test solution was replaced entirely with an identical volume of fresh solution twice every week, at an interval of alternate 3- and 4-day cycles, during the first 12 weeks. The frequency of solution replacement was later changed to once a week for the second 12-week period, followed by

replacement once every 2 weeks for the remaining test time. All experiments were continued for 1 year. Additional leaching tests were conducted at temperatures of 40 and 70 °C in the presence of FeCl<sub>2</sub> and FeCl<sub>3</sub> to determine dissolution kinetics of the two simulated high-level waste glasses. The test duration of these tests was 4 weeks, and the test solution was replaced with the same frequency used for the tests at 90 °C. At the end of each test period, the vessels were removed from the oven and allowed to cool. A small portion of the leachate was used to measure pH. The leachate was then filtered with a 0.45-µm syringe filter for cation analysis using the inductively coupled plasma atomic emission spectrometry technique.

The normalized concentration for element *i*,  $NC_i$ , and the normalized leach rate for element *i*,  $NLR_i$ , at the *n*<sup>th</sup> solution replacement can be calculated by the following equations:

$$NC_i = \frac{C_i}{F_i} \quad (3)$$

$$NLR_i = \frac{(NC_i)_n - (NC_i)_{n-1}}{\left(\frac{S}{V}\right)(t_n - t_{n-1})} \quad (4)$$

where

$NC_i$  — in units of g/m<sup>3</sup>

$C_i$  — concentration of element *i* in solution, in units of g/m<sup>3</sup>

$F_i$  — mass fraction of element *i* in glass (dimensionless)

$NLR_i$  — in units of g/m<sup>2</sup>•day

$t_n - t_{n-1}$  — time in days between the (n-1)<sup>th</sup> and *n*<sup>th</sup> solution replacements

$S/V$  — surface-to-volume ratio, in units of m<sup>-1</sup>

### 3. Results and discussion

#### 3.1 Effect of corrosion products on glass leaching

Leaching in the presence of iron chloride causes precipitates to form, especially in the high concentration solutions. Solid precipitates contained in the leachates were air-dried, and precipitate samples were then mounted on glass slides for x-ray diffraction analysis. X-ray diffraction patterns of the solid precipitates suggest the dominant occurrence of akaganeite ( $\beta$ -FeOOH) in all cases. Elemental chemical compositions of the precipitates were analyzed in scanning electron microscopy by energy-dispersive x-ray spectroscopy, and are shown in Table 3. Elemental oxygen was not included in the semiquantitative analysis. Contrary to the formation of iron silicate precipitates reported by McVay and Buckwalter [1] in both deionized water and J-13 groundwater in the presence of ductile iron, a very low silicon content was measured in the precipitates formed in the 0.25 M  $\text{FeCl}_3$  solution. A substantially higher silicon content, however, was detected in the 0.0025 M  $\text{FeCl}_3$  precipitates.

Results from the 1-year leaching program, which covered 51 solution replacements, are shown in Fig. 1 through 4. The accumulated  $NC_B$  results of the modified product consistency tests in various solutions are shown in Fig. 1 for WVDP Ref. 6 and the DWPF Blend 1 glasses, respectively. From Fig. 1, it is apparent that for both glasses the  $NC_B$  values in iron chloride solutions were consistently higher than those in deionized water, and leaching in 0.25 M  $\text{FeCl}_3$  solutions exhibited the highest boron release. The  $NC_B$  values of the leachates from the first solution replacement of the 0.25 M  $\text{FeCl}_3$  solution tests were observed to increase by factors of approximately 50 and 70 for these two glasses in comparison with those in deionized water. In addition, the accumulated  $NC_B$  is slightly higher in  $\text{FeCl}_3$  than in  $\text{FeCl}_2$  solutions and it is reached the constant value earlier, probably because of the lower pH of the  $\text{FeCl}_3$  solution. In an attempt to evaluate the effect of the solution pH, additional tests were performed for WVDP Ref. 6 glass in 0.25 M HCl solutions. As shown in Table 2, the initial pH of the 0.25 M  $\text{FeCl}_3$  solution is higher than that of 0.25 M HCl. The leaching results in 0.25 M HCl are also included in Fig. 1. Although a factor of 30 increase in  $NC_B$  was measured

from the first solution replacement, compared to the deionized water result, the total  $NC_B$  in 0.25 M HCl was only approximately half that in 0.25 M  $FeCl_3$ .

The  $NLR_B$  results were also calculated using Eq. (4) and are shown in Fig. 2 for WVDP Ref. 6 and DWPF Blend 1 glasses, respectively. It is apparent that the initial  $NLR_B$  values were much higher than the steady state values in the high concentration iron chloride solution tests. In all cases,  $NLR_B$  decreased with time, but this tendency is much greater in 0.25 M  $FeCl_3$  solutions. Also, the  $NLR_B$  was generally higher in the presence of iron chloride in comparison with that in deionized water except in high concentration chloride solutions after prolonged leaching. The substantially low  $NLR_B$  values observed for WVDP Ref. 6 glass in 0.25 M  $FeCl_3$  solution after only 10 days of leaching are in agreement with the evidence of leveling off of the  $NC_B$  after the same leaching period, as shown in Fig. 1. For the  $NLR_{Si}$  results for WVDP Ref. 6 glass in various solutions in all cases,  $NLR_{Si}$  remained almost constant throughout the leaching duration. The  $NLR_{Si}$  levels depend on the test solution. Higher silicon release rates were measured in the high concentration iron chloride solution tests. The normalized release rates for various elements are shown in Fig. 3 for WVDP Ref. 6 glass in 0.25 M  $FeCl_3$  solution. Figure 3 indicates that all elements undergo congruent dissolution during the initial period of 24 days with the exception of silicon and aluminum after 17 days of leaching. DWPF Blend 1 glass also showed a similar trend.

The initial and final pH values of various leachates from WVDP Ref. 6 glass are shown in Fig. 4. In all cases, except the leachates from the high concentration iron chloride solution tests at each solution replacement, the final pH values were generally higher than the initial. Variations in solution pH showed that, while the pH of the leachates from high concentration iron chloride solutions changed slightly and remained acidic throughout the leaching duration, it substantially increased in all the deionized water and low concentration iron chloride tests. It is interesting to observe that after the initial period of 80 days, the final pH in the dilute iron chloride solutions reached almost a constant value. Similar changes in leachate pH were also observed for DWPF Blend 1 glass. In

addition, leaching in deionized water showed high elemental releases in the SRL EA glass as a result of a higher leachate pH ( $\approx 11.6$ ) in comparison with two other glasses ( $\text{pH} \approx 10.2$ ).

WVDP Ref. 6 glasses, both before and after leaching, were analyzed to determine their morphology and chemical composition using scanning electron microscopy. Figure 5 shows representative micrographs of WVDP Ref. 6 glass particles before leaching and after leaching in deionized water and in 0.25 M  $\text{FeCl}_3$  solution. As shown in Fig. 5, while the surface of the starting glass particles was clean, the leaching process formed surface layers and precipitates on the particle facets. It is also noted that after leaching in the 0.25 M  $\text{FeCl}_3$  solution, the particle size of WVDP Ref. 6 glass was significantly reduced. In contrast, the particle size remained essentially unchanged after leaching in deionized water, but evidence of attack can be seen on the glass surfaces. Fragmentation of WVDP Ref. 6 glass in 0.25 M  $\text{FeCl}_3$  solution may be attributed to a combined effect of chemical dissolution and mechanical breakdown as a result of thermal stresses induced during periodic solution replacements. The chemical composition using the energy-dispersive x-ray spectroscopy analysis from the near surface regions of these three corresponding glass conditions is presented in Table 4. The absence of light elements (i.e., lithium and boron) was due to the detection limits of the instrument. Variations of the glass chemistry in relation to leaching conditions were observed. While sodium was substantially less in the deionized water leached glass, all alkali elements were completely removed from the 0.25 M  $\text{FeCl}_3$  leached glass. These near surface glass chemistry variations are consistent with the leachate analyses discussed previously.

The reaction of borosilicate glasses with aqueous solutions generally includes two independent processes: initial diffusion-controlled extraction of alkali ions out of the glass matrix, and the dissolution of the glass matrix itself. The initial reaction causing alkali release is commonly known as an ion-exchange process which results from water diffusing into the glass network. As the

release rate decreases with increasing depth of the alkali depletion zone in the outer glass surface, matrix-dissolution becomes the dominant reaction.

The results from this study indicate that leachant pH is a dominant factor in the leaching of simulated waste glasses. At the beginning of the tests, the hydronium ion ( $\text{H}_3\text{O}^+$ ) in solution tends to exchange with the alkalis in the glass matrix through the ion-exchange reaction. The more acidic the test solution, the faster the alkali release rates. This theory is supported by the inductively coupled plasma atomic emission spectrometry analyses shown in Fig. 2. It is also expected that the ion-exchange reaction consumes hydronium ions and releases alkalis from the glass matrix. As a result, the leachate pH is anticipated to increase at the end of glass leaching. In the case of glass dissolution in 0.25 M  $\text{FeCl}_3$  solution, an increase of the leachate pH, accompanied by the highest alkali release, was measured for the initial solution replacements (Fig. 3 and 4). However, as the alkali release substantially reduced, the leachate pH was also observed to decrease for the rest of the solution replacements. The effect is clearly noticeable in the 0.0025 M  $\text{FeCl}_2$  and 0.0025 M  $\text{FeCl}_3$  solutions in which a steady decrease of the final pH can be observed during the initial 80-day replacement period. From the glass surface analysis results, it is apparent that the high initial leaching resulted in the formation of an alkali-depleted surface layer, and consequently, the leaching rate decreased as a result of the extended diffusion path.

The mechanism by which Fe cations (both  $\text{Fe}^{3+}$  and  $\text{Fe}^{2+}$ ) accelerate the glass leaching process is not clear. The formation of iron silicate precipitates that inhibit saturation effects is generally speculated to enhance glass dissolution in the presence of iron products [1]. The results from this study, however, do not support this speculation. As reported in this study, even though leachate pH has a profound effect on glass dissolution, the leaching rate measured from the first solution replacement in 0.25 M  $\text{FeCl}_3$  solution was almost twice that in the 0.25 M HCl solution. These results suggest that both solution pH and the presence of corrosion species such as iron chloride are significant contributing factors to the net glass durability.

### 3.2 Dissolution kinetics and model abstraction

As can be seen from Fig. 2, the glass leaching results show the characteristic initial rapid leach rates that provide a conservative account of the effect of glass dissolution. Leach rates calculated after the first solution replacement are plotted as a function of leachate pH in Fig. 6 for WVDP Ref. 6 and DWPF Blend 1 glasses at temperatures of 40, 70, and 90 °C. The initial leach rates for all major components were pH dependent. While the leach rates for boron and alkali decreased with an increase in pH, the silicon release rate remained relatively constant. The aluminum leach rate showed a minimum for both the 70 and 90 °C tests. The pH value at which the minimum rate occurred varied with both the glass composition and test temperature. For the 40 °C tests, however, the leach rates for all elements decreased continuously with increasing leachate pH. Figure 7 shows the  $\log NLR_B$  as a function of leachate pH at each temperature for both WVDP Ref. 6 and DWPF Blend 1 glasses, based on the initial release of boron. A linear regression between  $\log NLR_B$  and leachate pH was performed, and the regression equations are also given in Fig. 7. A good correlation between leach rate and pH is found for all test temperatures as indicated by the reasonable high correlation coefficients ( $R^2$ ).

In contrast to a linear pH dependence with a negative slope observed for boron release in this study, Knauss, et al. [9] and Abraitis, et al. [10] conducted experiments in controlled pH environments and reported a V-shaped dissolution rate versus pH curves with minima at near-neutral pH for both boron and silicon releases. McGrail, et al. [11] also studied glass dissolution kinetics at pH values between 6 and 12 and showed that glass dissolution increases with increasing pH. These observations suggest that the effect of pH on glass dissolution depends on the glass compositions and test conditions. While all the experiments in the cited references were conducted in controlled pH environments in the absence of the influence of the affinity term, solution pH was initially set by hydrolysis of  $FeCl_2$  or  $FeCl_3$  in this study, and the final pH values were generally higher than the initial ones. In the case of glass leaching in deionized water, the leachate

pH drifted from acidic to the basic range. The observed discrepancy in the effect of pH on dissolution rate in the basic range could be the result of variations in leachate pH. It is also noted that the initial leach rates for boron and most alkali elements are much higher in comparison with the silicon release rate in the low pH ranges. High-level waste glass dissolution rates could be significantly underestimated if based on measured silicon release rates. In addition, the influence of the affinity term has not been evaluated under the current test conditions. Nevertheless, the use of boron release rates provides a conservative upper bound to the release rate of radionuclides because boron is released at a rate similar to alkali ions and is not incorporated into secondary phases similar to Tc-99.

The slopes of the linear regression equations plotted in Fig. 7 provide the pH dependence coefficients ( $\eta$ ). It is apparent that  $\eta$  does not significantly change with the test temperature and glass composition. Activation energy ( $E_a$ ) can be regressed from the experimental data by plotting  $\ln NLR_B$  versus  $1/T$  based on the rate equation in Eq. (2), and the effective rate constant ( $k_{eff}$ ) can then be determined using the values of  $\eta$  and  $E_a$ . The model parameters are summarized in Table 5. The  $E_a$  values for both waste glasses are consistent with the values reported in the literature for borosilicate waste glasses [9-12]. The mean and standard deviation values calculated for a combined case are listed in Table 6 (Case A) and compared to the bounding parameter values (Case B) adopted by the DOE [13]. Note that the rate expression used by the DOE for the basic leg has combined the affinity term with the intrinsic dissolution rate constant. A significantly higher  $k_0$  value,  $\log_{10} k_0 = 7.91 \pm 0.16$ , was measured from the forward rates by conducting MCC-1 tests [13]. In addition to the effect of the affinity term, the effective rate constants measured in this study would also include another term that accounts for the effect of corrosion products.

It is also noted that the results listed in Tables 5 and 6 (Case A) were obtained using the final pH values of the leachates from first solution replacement. Since solution pH changes during the leaching test, the final pH values may not be representative of the pH during the course of the

experiment. An average of the initial and final pH values would be more realistic in the absence of pH measurements during exposure. The model parameters calculated using average pH values are also listed in Table 6 (Case A').

The rate expression for dissolution of waste glasses has been evaluated by the DOE [13] primarily based on the experimental results by Knauss, et al. [9]. Because the glass dissolution rates were found to have a V-shaped pH dependence, with minima at near-neutral pH, separate rate expressions were obtained for dissolution under acidic or base conditions, as reflected in Table 6 (Case B). In addition, the release of boron occurred faster than that of silicon under some test conditions. The model parameter values based on boron release rates were determined to bound the range of high-level waste glass compositions and environmental conditions. The calculated dissolution rates on the basis of Eq. (2) and various model parameters in Table 6 are compared in Fig. 8. It is seen that the model parameters supported by the current experimental data are associated with higher dissolution rates in the near-neutral pH range than those reported by the DOE. Considering the dissolution behavior in the alkaline range reported by the DOE [13], the rate expression based on average pH leads to closer agreement with the DOE results in the absence of leaching tests with the initial pH in the alkaline region. Nevertheless, the higher dissolution rates are consistent with the observations of enhanced glass dissolution in the presence of iron-containing corrosion products.

### 3.3 Performance assessment estimation

The U.S. Nuclear Regulatory Commission (NRC) and CNWRA have been developing a tool, the Total-system Performance Assessment code [14], intended to support review activities for a potential license application by the DOE for construction of a high-level waste repository at Yucca Mountain. Based on a Monte Carlo scheme, the Total-system Performance Assessment code is used to compute the expected annual total effective dose equivalent to the reasonably maximally exposed individual in the event of failure of the waste packages to isolate radionuclides. A nominal

case (defined as a particular set of models and model parameters describing likely behaviors of the proposed repository system) is generally selected to perform sensitivity and uncertainty analyses and to study the performance of the system as simulated by the code. In the nominal case model or description, it is assumed that 70,040 metric tons of heavy metal of spent nuclear fuel is packaged in 7,176 waste packages and emplaced in the proposed repository. Each waste package contains, on average, 9.8 metric tons of spent nuclear fuel. The nominal case description does not account for the presence of high-level waste in glass form. Equation (2) was incorporated into the code to account for glass leaching in the event glass is contacted by water. Computations presented in this section are aimed at evaluating the relative importance of glass dissolution, in units of dose, with respect to spent nuclear fuel dissolution.

In the computer simulations, the model parameters obtained from this work (Case A) and from the DOE (Case B) in Table 6 were considered. The current Total-system Performance Assessment Code Version 4.1 does not allow for the simultaneous inclusion of two waste forms in the estimation of the dose. To circumvent that problem, it was assumed that glass was the only kind of waste form in the system and that a total of 4,667 metric tons of heavy metal of high-level waste glass [6] is contained in 3,910 waste packages was emplaced in the proposed repository [15]. The initial radionuclide inventory was selected from available data [15]. To obtain appropriate comparisons of the dose derived from glass dissolution to the nominal case dose, a temperature-versus-time curve for the latter case was employed. The justification is that in the mixed system, spent nuclear fuel and glass waste forms, the temperature of the repository is dictated by the thermal activity of the spent nuclear fuel. The total surface area of the exposed glass waste form per waste package was set equal to 99 m<sup>2</sup>, as suggested by other studies [16]. In the Monte Carlo analysis, the pH was uniformly sampled in the range 4.8 to 10, consistent with predictions of the chemistry inside the waste package [17]. Results of the computations are summarized in Fig. 9.

The mean dose rates for these runs were computed by averaging the total effective dose equivalent for the nominal scenario at an instant of time from 200 Monte Carlo realizations and are plotted in Fig. 9 for each case. As shown in Fig. 9, the predicted mean dose rates for Case A are higher than those computed for Case B (Cases A and B refer to the notation in Table 6), which are a direct consequence of the higher dissolution rates in the near-neutral pH associated to Case A that accounts for the effect of corrosion products (see Fig. 8). The impact of glass dissolution on the predicted mean dose rate in Case A could be up to 30 percent of the nominal case at times of the order of 52,000 years. Within the first 10,000 years, the dose deriving from glass dissolution is of the same order of magnitude as the nominal case dose. Nevertheless, the magnitude of these predicted mean dose rates is less than  $10^{-3}$  rem/yr at times  $t < 60,000$  years, as shown in Fig. 9. The dose at earlier times are a consequence of the assumption that initial defects could be present in waste containers. At times greater than 40,000 years, a significant number of waste packages would fail caused by general corrosion; thus, additional sources of radionuclide release would be available in the system, causing the increase in the dose. Figures 9 and 11 present the corresponding release rates of various radionuclides for the nominal case and Case A, respectively. As evident in both figures, while Np-237 is the predominant radionuclide contributing to the mean dose rate at all times, Tc-99 and I-129 are significant contributors at early times ( $< 15,000$  years) because of their high solubility in the water contacting the waste form.

#### **4. Conclusions**

The DOE model abstraction for high-level waste glass degradation ignores the presence of corrosion products from the dissolution of waste package internal components, such as FeOOH, FeCl<sub>2</sub>, and FeCl<sub>3</sub>, that could influence glass degradation. To evaluate the effects of corrosion products on degradation of waste form and subsequent release of radionuclides to the environment, we have conducted leaching experiments of simulated high-level waste glasses in aqueous solutions of FeCl<sub>2</sub> and FeCl<sub>3</sub> resembling the internal waste package environments. Rate

expressions for glass dissolution that account for the effects of corrosion products were developed and used to evaluate the impact of glass waste form on radionuclide release within the context of a performance assessment for the proposed geologic repository at Yucca Mountain, Nevada.

Leaching experiments showed that substantially high initial boron and alkali release rates, approximately 50 to 70 times greater than those in deionized water, were measured in 0.25 M FeCl<sub>3</sub> solutions. The calculated dissolution rates on the basis of various rate expressions indicate that model parameters supported by the current experimental data are associated with higher dissolution rates in the near-neutral pH range than those reported by the DOE. The calculated results are consistent with the observations of enhanced glass dissolution in the presence of iron-containing corrosion products. Performance assessment calculations of the high-level waste glass cases and the spent fuel nominal case for the proposed repository showed that the impact of glass dissolution on the predicted mean dose rate could be up to 30 percent of the nominal case at times of the order of 52,000 years.

### **Acknowledgments**

The authors gratefully acknowledge S.T. Clay and J.F. Spencer for conducting leaching experiments, x-ray diffraction, and scanning electron microscopy analyses. Thanks are also due to D. Ramirez and J.M. Ranger for cation analyses by inductively coupled plasma atomic emission spectrometry. This article was prepared to document the work performed by the CNWRA for the NRC under contract No. NRC-02-97-009. This article is an independent product of the CNWRA and does not necessarily reflect the views or the regulatory position of the NRC.

### **References**

- [1] G.L. McVay and C.Q. Buckwalter, *J. Am. Ceram. Soc.* 66 [3] (1983) 170.
- [2] D.B. Burns, B.H. Upton, and G.G. Wicks, *J. Non-Cryst. Solids* 84 (1986) 258.
- [3] Y. Inagaki, A. Ogata, H. Furuya, K. Idemitsu, T. Banba, and T. Maeda, *Mat. Res. Soc. Symp. Proc.*, Vol. 412 (1996) 257.

- [4] G. Bart, H.U. Zwicky, E.T. Aerne, TH. Graber, D. Z'Berg, and M. Tokiwai, *Mat. Res. Soc. Symp. Proc.*, Vol. 84 (1987) 459.
- [5] L. Werme, I.K. Bjorner, G. Bart, H.U. Zwicky, B. Grambow, W. Lutze, R.C. Ewing, and C. Magrabi, *J. Mat. Res.* 5 [5] (1983) 1130.
- [6] U.S. Department of Energy Report TDR–WIS–MD–000001, Rev. 00, ICN 01, Civilian Radioactive Waste Management System, Las Vegas, NV, 2000.
- [7] U.S. Department of Energy Report TDR–WIS–PA–000001, Rev. 00, ICN 01, Civilian Radioactive Waste Management System, Las Vegas, NV, 2000.
- [8] American Society for Testing and Materials, *Standard Test Methods for Determining Chemical Durability of Nuclear, Hazardous, and Mixed Waste Glasses: the Product Consistency Test (PCT)*, C1285-97, American Society for Testing and Materials, West Conshohocken, PA, 1999.
- [9] K.G. Knauss, W.L. Bourcier, K.D. McKeegan, C.I. Merzbacher, S.N. Nguyen, F.J. Ryerson, D.K. Smith, H.C. Weed, and L. Newton, *Mat. Res. Soc. Symp. Proc.*, Vol. 176 (1990) 371.
- [10] P.K. Abraitis, D.J. Vaughan, F.R. Livens, L. Monteith, D.P. Trivedi, and J.S. Small, *Mat. Res. Soc. Symp. Proc.*, Vol. 506 (1998) 47.
- [11] B.P. McGrail, W.L. Ebert, A.J. Bakel, and D.K. Peeler, *J. Nucl. Mat.* 249 (1997) 175.
- [12] T. Advocat, J.L. Crovisier, E. Vernaz, G. Ehret, and H. Charpentier, *Mat. Res. Soc. Symp. Proc.*, Vol. 212 (1991) 57.
- [13] U.S. Department of Energy Report ANL–EBS–MD–000016, Rev. 00, ICN 01, Civilian Radioactive Waste Management System, Las Vegas, NV, 2000.
- [14] S. Mohanty and T.J. McCartin, *Total-system Performance Assessment (TPA) Version 4.0 Code: Module Description and User's Guide*, Center for Nuclear Waste Regulatory Analyses, San Antonio, TX, 2000.
- [15] U.S. Department of Energy Report ANL–WIS–MD–000006, Rev. 00, Civilian Radioactive Waste Management System, Las Vegas, NV, 2000.

- [16] U.S. Department of Energy Report B00000000-01717-4301-00006, Rev. 01, Civilian Radioactive Waste Management System, Las Vegas, NV, 1998.
- [17] U.S. Department of Energy Report ANL-EBS-MD-000050, Rev. 00, Civilian Radioactive Waste Management System, Las Vegas, NV, 2000.

Table 1. Chemical compositions of test glasses (in weight percent)

Oxide Compound	SRL EA Glass*	WVDP Ref. 6 Glass <sup>†</sup>	DWPF Blend 1 Glass <sup>‡</sup>
Al <sub>2</sub> O <sub>3</sub>	3.60	6.67	4.16
B <sub>2</sub> O <sub>3</sub>	11.16	11.48	8.05
BaO	—	—	0.18
CaO	1.23	0.66	1.03
Cr <sub>2</sub> O <sub>3</sub>	—	—	0.13
Cs <sub>2</sub> O	—	—	0.08
CuO	—	—	0.44
FeO	1.59	—	—
Fe <sub>2</sub> O <sub>3</sub>	7.58	11.95	10.91
K <sub>2</sub> O	0.04	5.15	3.68
La <sub>2</sub> O <sub>3</sub>	0.28	—	—
Li <sub>2</sub> O	4.21	4.84	4.44
MgO	1.79	0.18	1.41
MnO	1.36	0.51	—
MnO <sub>2</sub>	—	—	2.05
MoO <sub>3</sub>	—	—	0.15
Na <sub>2</sub> O	16.88	11.94	9.13
Nd <sub>2</sub> O <sub>3</sub>	—	—	0.22
NiO	0.53	—	0.89
P <sub>2</sub> O <sub>5</sub>	—	2.01	—
RuO <sub>2</sub>	—	—	0.03
SO <sub>3</sub>	—	0.25	—
SiO <sub>2</sub>	48.76	42.28	51.9
TiO <sub>2</sub>	0.65	1.04	0.89
ZnO	0.26	—	—
ZrO <sub>2</sub>	0.48	1.28	0.14
Total	100.40	100.24	99.91

\*C.M. Jantzen, N.E. Bibler, D.C. Crawford, and M.A. Pickett. "Characterization of the Defense Waste Processing Facility (DWPF) Environmental Assessment (EA) Glass Standard Reference Material (U)." WSRC-TR-92-346. Aiken, South Carolina: Westinghouse Savannah River Company. 1993.

<sup>†</sup>Composition provided by West Valley Nuclear Services Company, Inc.

<sup>‡</sup>Composition provided by Westinghouse Savannah River Company.

Table 2. Glass leaching solution test matrix

Test Solution	Glass Type	Initial pH
Deionized Water	—	5.78
Deionized Water	SRL EA	5.78
Deionized Water	WVDP Ref. 6	5.78
0.0025 M FeCl <sub>2</sub>	WVDP Ref. 6	3.95
0.0025 M FeCl <sub>3</sub>	WVDP Ref. 6	2.22
0.25 M FeCl <sub>2</sub>	WVDP Ref. 6	2.47
0.25 M FeCl <sub>3</sub>	WVDP Ref. 6	1.34
0.25 M HCl	WVDP Ref. 6	0.69
Deionized Water	DWPF Blend 1	5.78
0.0025 M FeCl <sub>2</sub>	DWPF Blend 1	3.95
0.0025 M FeCl <sub>3</sub>	DWPF Blend 1	2.22
0.25 M FeCl <sub>2</sub>	DWPF Blend 1	2.47
0.25 M FeCl <sub>3</sub>	DWPF Blend 1	1.34

Table 3. Chemical compositions of precipitates from leaching of WVDP Ref. 6 glass in various solutions (in weight percent)

Test Solution	Al	Fe	K	Na	P	Si	Ti	S	Cl	Mn
0.0025 M FeCl <sub>3</sub>	6.2	48.9	4.9	4.7	2.1	28.1	0.9	0.3	1.7	0.9
0.25 M FeCl <sub>2</sub>	0.7	77.9	0.3	1.6	0.3	1.7	—	—	17.4	—
0.25 M FeCl <sub>3</sub>	0.4	76.7	—	—	0.6	0.6	—	1.1	20.6	—

Table 4. Chemical compositions from surface regions of WVDP Ref. 6 glass before and after leaching (in weight percent)

Test Solution	Al	Fe	K	Na	P	Si	Ti	Zr	Cl	O
Before Leaching	5.2	2.7	3.0	11.1	1.1	22.8	0.4	3.4	—	50.2
Deionized Water	5.0	8.6	5.7	3.5	1.3	32.2	0.9	4.6	—	37.0
0.25 M FeCl <sub>3</sub>	1.6	5.6	—	—	—	45.2	0.4	6.9	1.8	38.5

Table 5. Glass dissolution model parameters summary

Glass	Temperature (°C)	$\log_{10} k_{\text{eff}}^*$	$\eta$	$E_a$ (kJ/mol)
WVDP Ref. 6	40	8.53	-0.2345	
WVDP Ref. 6	70	8.57	-0.2260	$49.2 \pm 7.4$
WVDP Ref. 6	90	8.22	-0.1789	
DWPF Blend 1	40	8.49	-0.1894	
DWPF Blend 1	70	8.60	-0.2026	$52.8 \pm 2.5$
DWPF Blend 1	90	8.37	-0.1780	

\*For  $k_{\text{eff}}$  in  $\text{g}/\text{m}^2 \cdot \text{day}$

Table 6. Comparison of glass dissolution model parameters

Parameter	Case A (CNWRA Rate Expression —Final pH)	Case A' (CNWRA Rate Expression —Average pH)	Case B (DOE Rate Expression)
$k_{\text{eff}}$ (g/m <sup>2</sup> •day)	$10^{8.46 \pm 0.14}$	$10^{7.49 \pm 0.10}$	$10^{14.0 \pm 0.5}$ if pH < 7.1 $10^{6.9 \pm 0.5}$ if pH ≥ 7.1
$\eta$	$-0.20 \pm 0.02$	$-0.27 \pm 0.02$	$-0.6 \pm 0.1$ if pH < 7.1 $0.4 \pm 0.1$ if pH ≥ 7.1
$E_a$ (kJ/mol)	$51.0 \pm 5.6$	$44.4 \pm 2.6$	$80 \pm 10$ if pH < 7.1 $80 \pm 10$ if pH ≥ 7.1

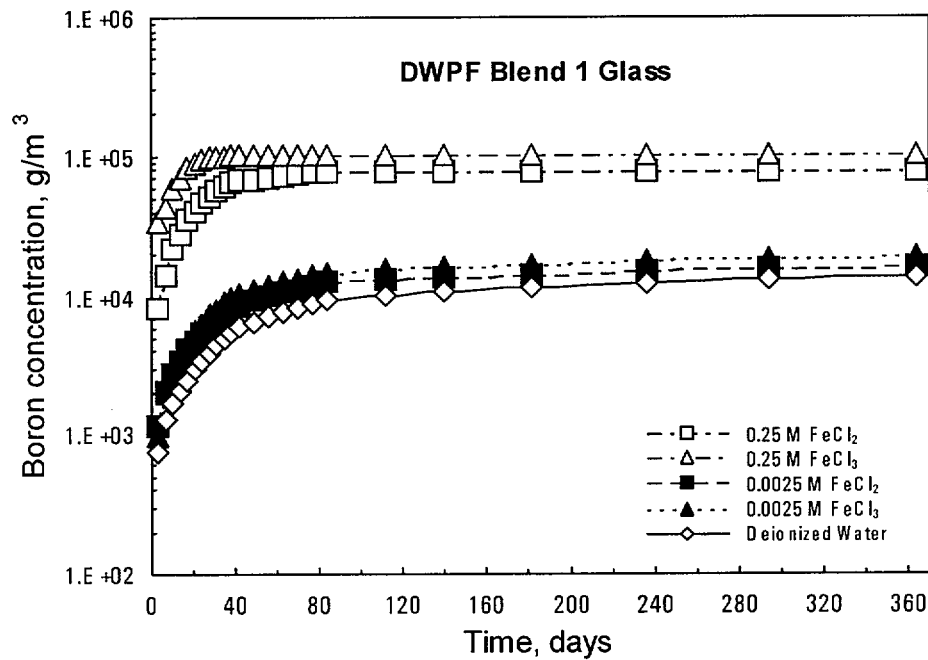
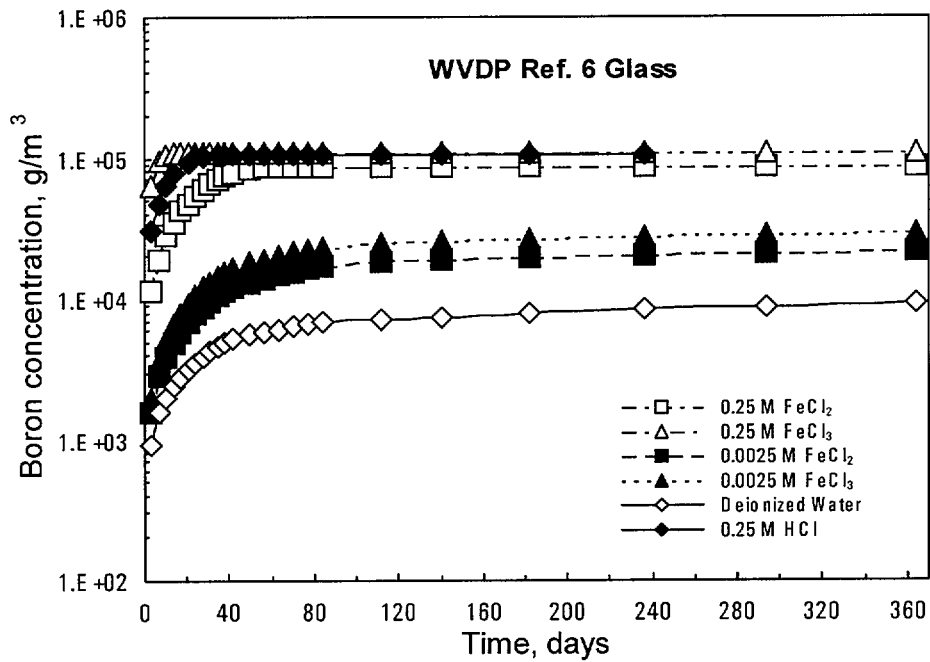


Fig. 1. The accumulated normalized concentration for boron versus time for WVDP Ref. 6 and DWPF Blend 1 glasses in various solutions at 90 °C

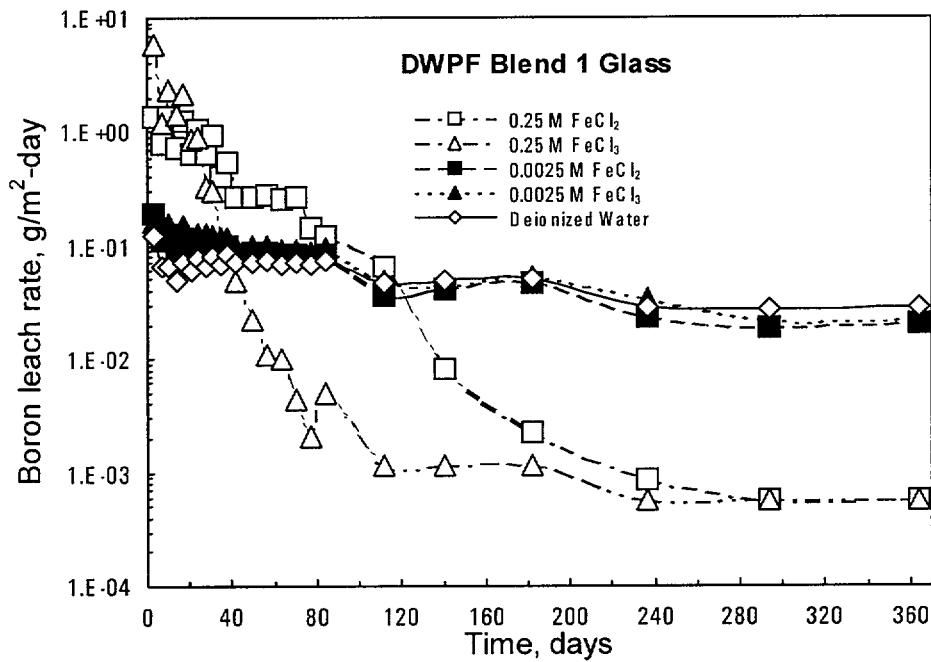
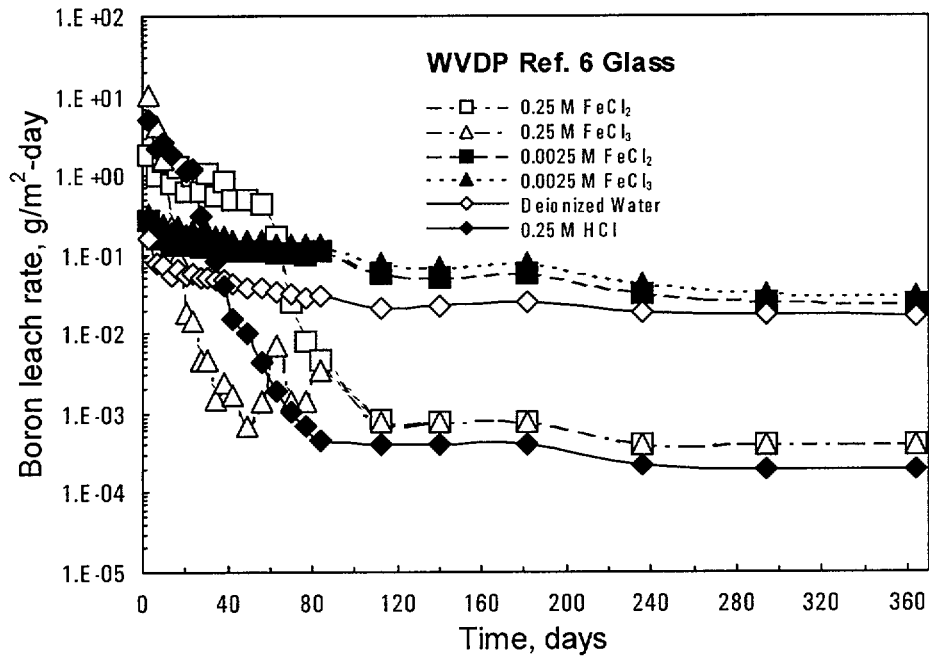


Fig. 2. Normalized leach rate for boron versus time for WVDP Ref. 6 and DWPF Blend 1 glasses in various solutions at 90 °C

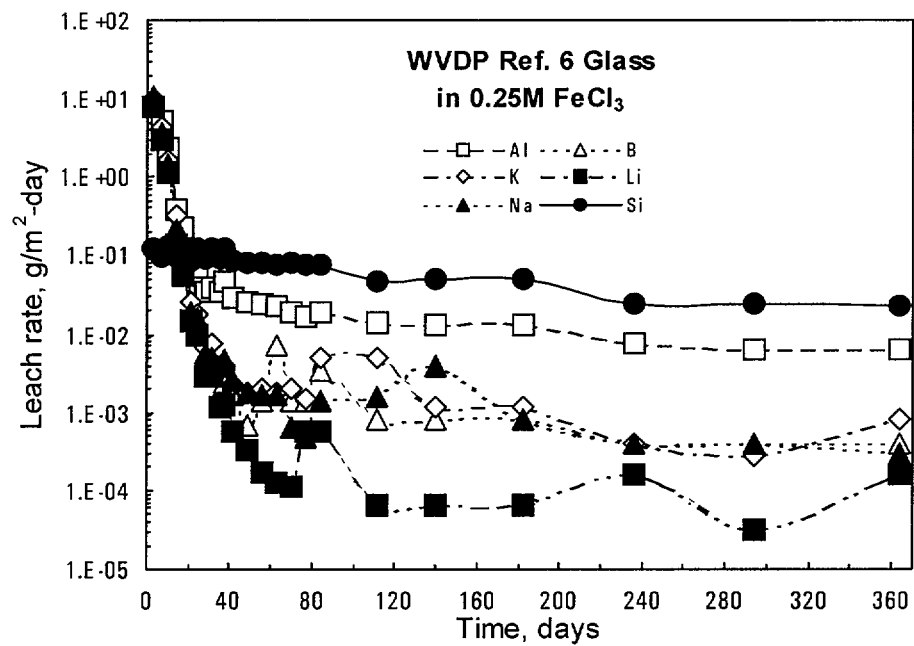


Fig. 3. Normalized leach rates for various elements as a function of time for WVDP Ref. 6 glass in 0.25 M FeCl<sub>3</sub> solution at 90 °C

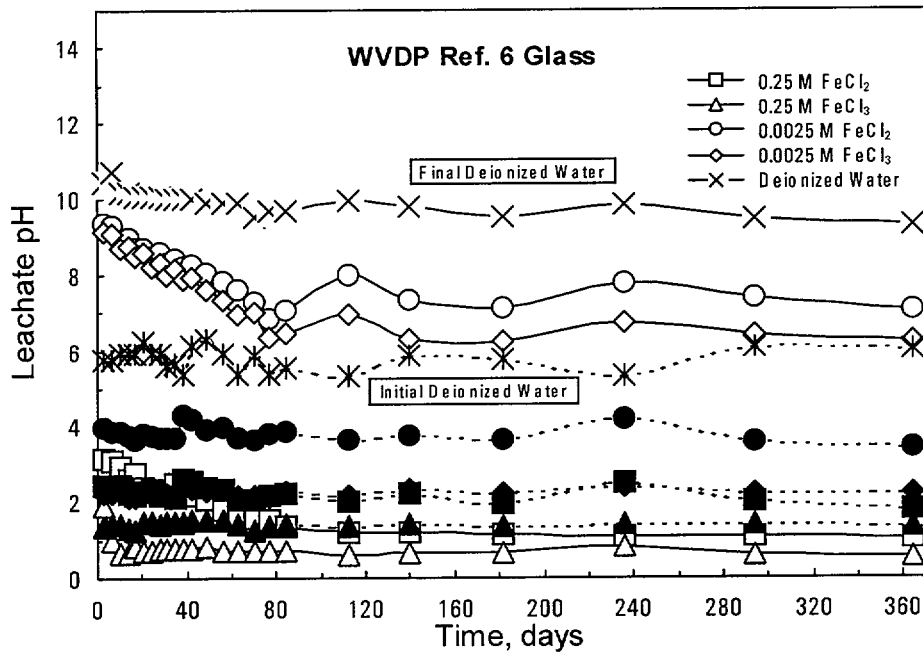


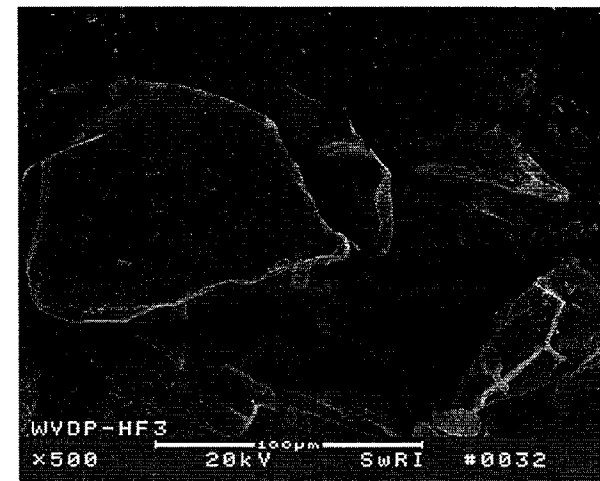
Fig. 4. Leachate pH versus time for WVDP Ref. 6 glass in various solutions at 90 °C (Closed symbols for the initial pH and open symbols for the final pH)



(a)



(b)



(c)

Fig. 5. Scanning electron micrographs of WVD glass (a) before leaching and after leaching in (b) deionized water and (c) 0.25 M FeCl<sub>3</sub> solution at 90 °C

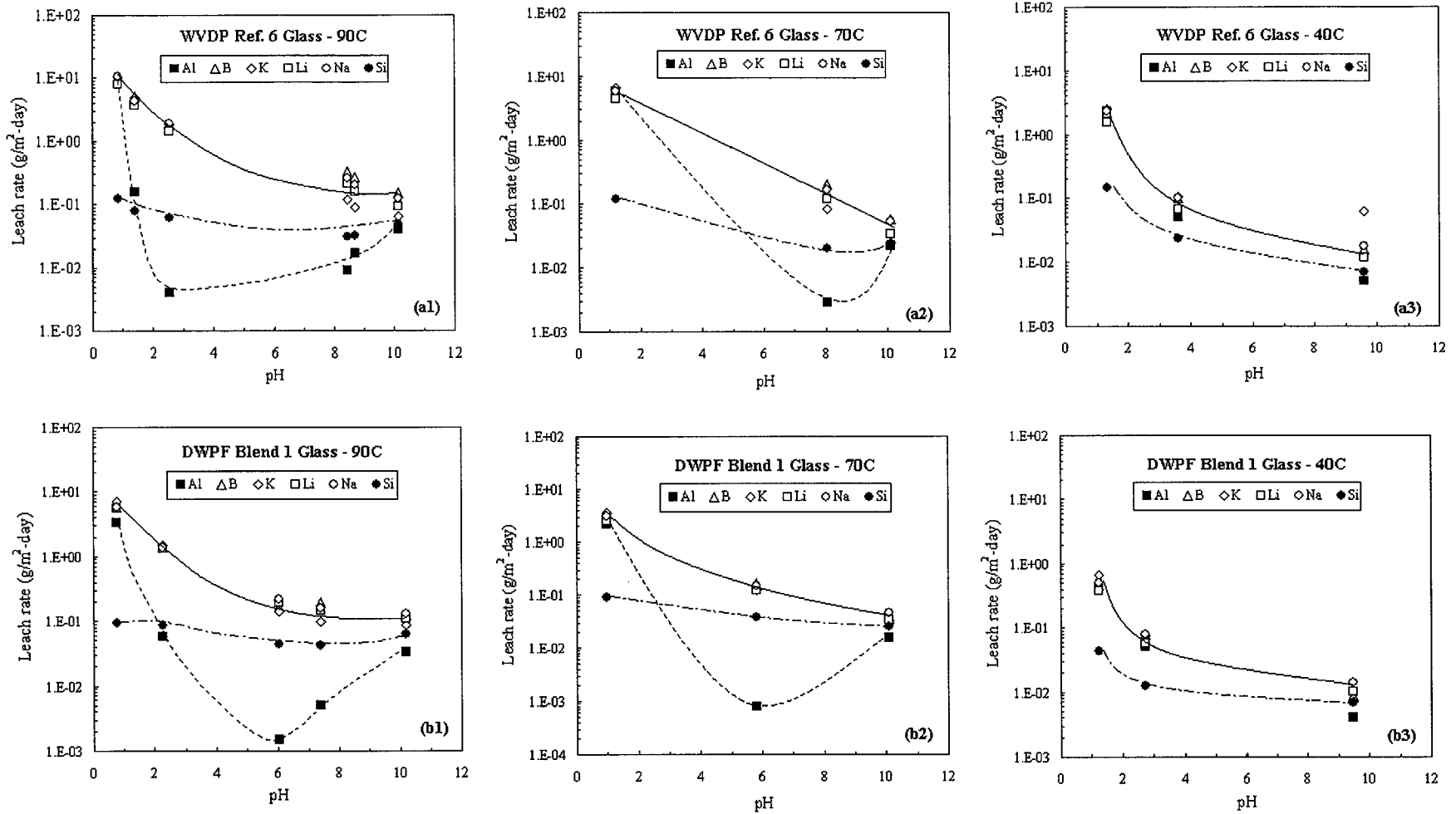


Fig. 6. Normalized leach rate for various elements versus leachate pH after first solution replacement for (a) WVDP and (b) DWPF glasses at various temperatures

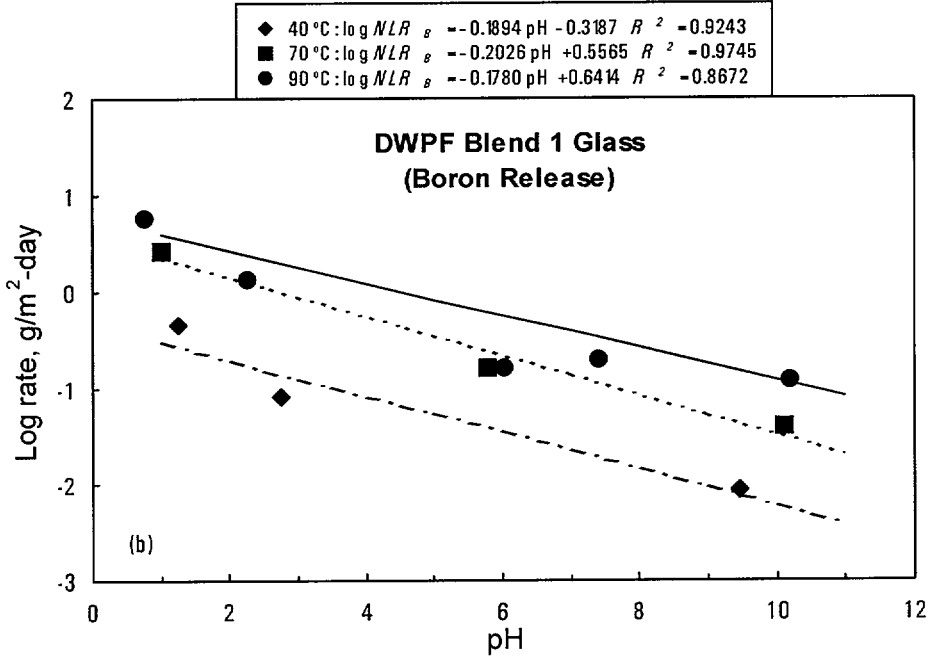
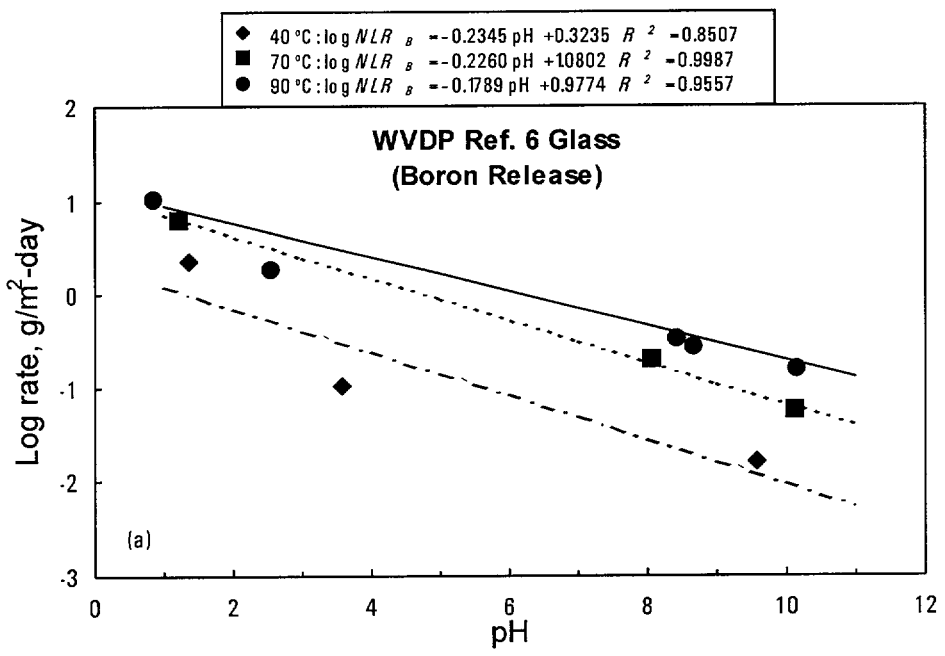


Fig. 7. Linear regression of normalized leach rate for boron versus leachate pH after first solution replacement for (a) WVDP Ref. 6 and (b) DWPF Blend 1 glasses at various temperatures

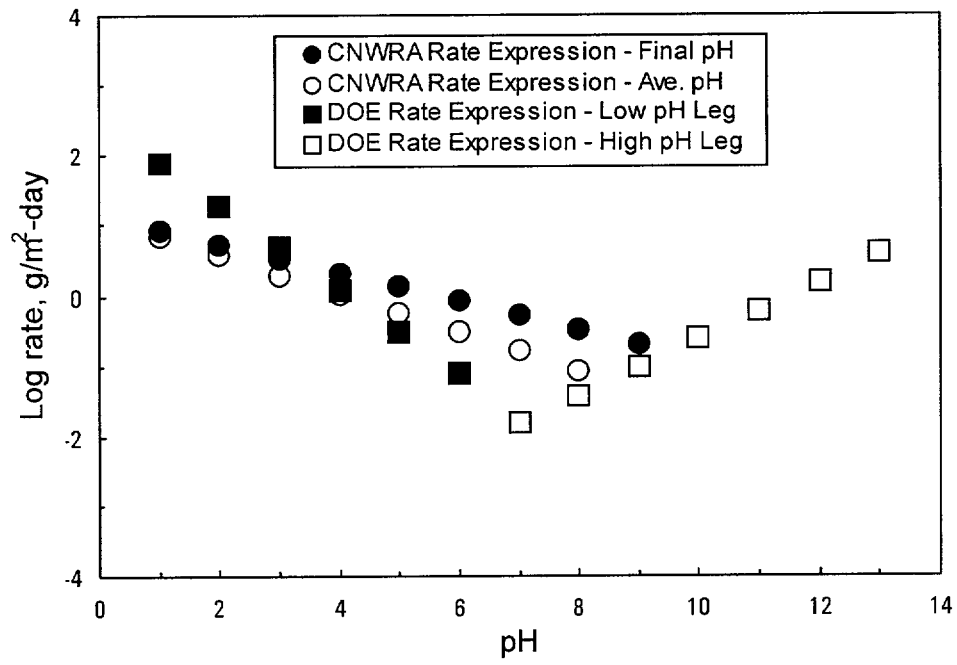


Fig. 8. Comparison of calculated glass dissolution rates using different rate expressions

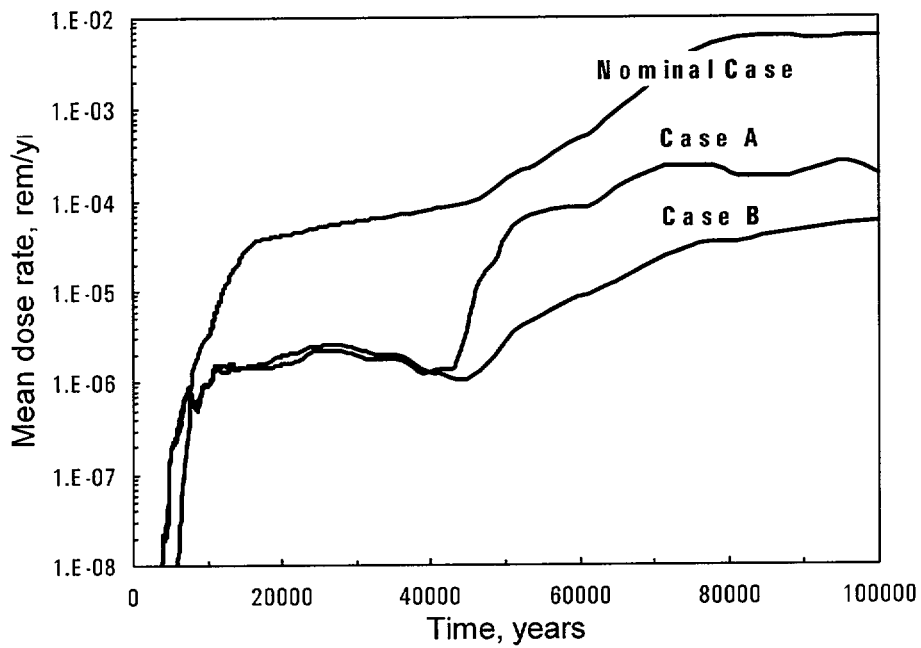


Fig. 9. Calculated mean dose rates for three cases from 200 realizations. The Cases A and B that account for 4,667 metric tons of heavy metal of high-level waste glass refer to the parameters in Table 6. The nominal case of the Total-system Performance Assessment code models 70,040 metric tons of heavy metal of spent nuclear fuel in the repository system.

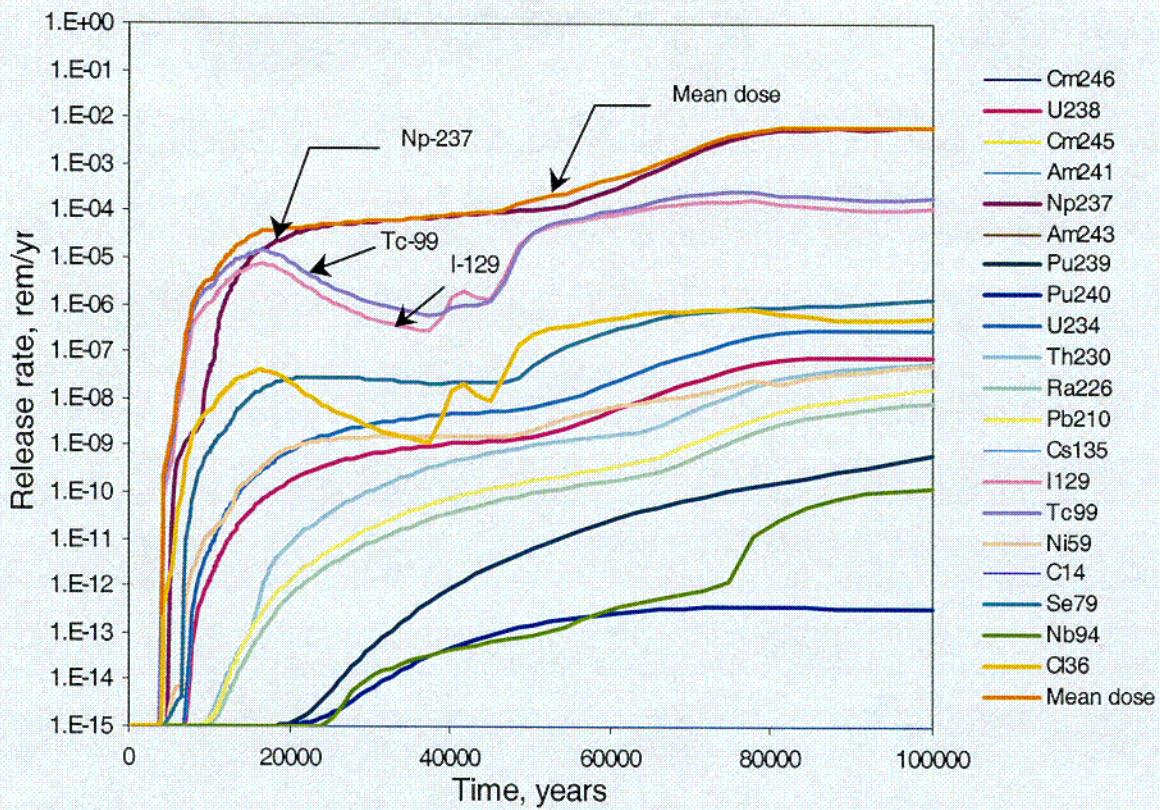


Fig. 10. Calculated release rates for various radionuclides for the nominal case from 200 realizations. The nominal case of the Total-system Performance Assessment code models 70,040 metric tons of heavy metal of spent nuclear fuel in the repository system.

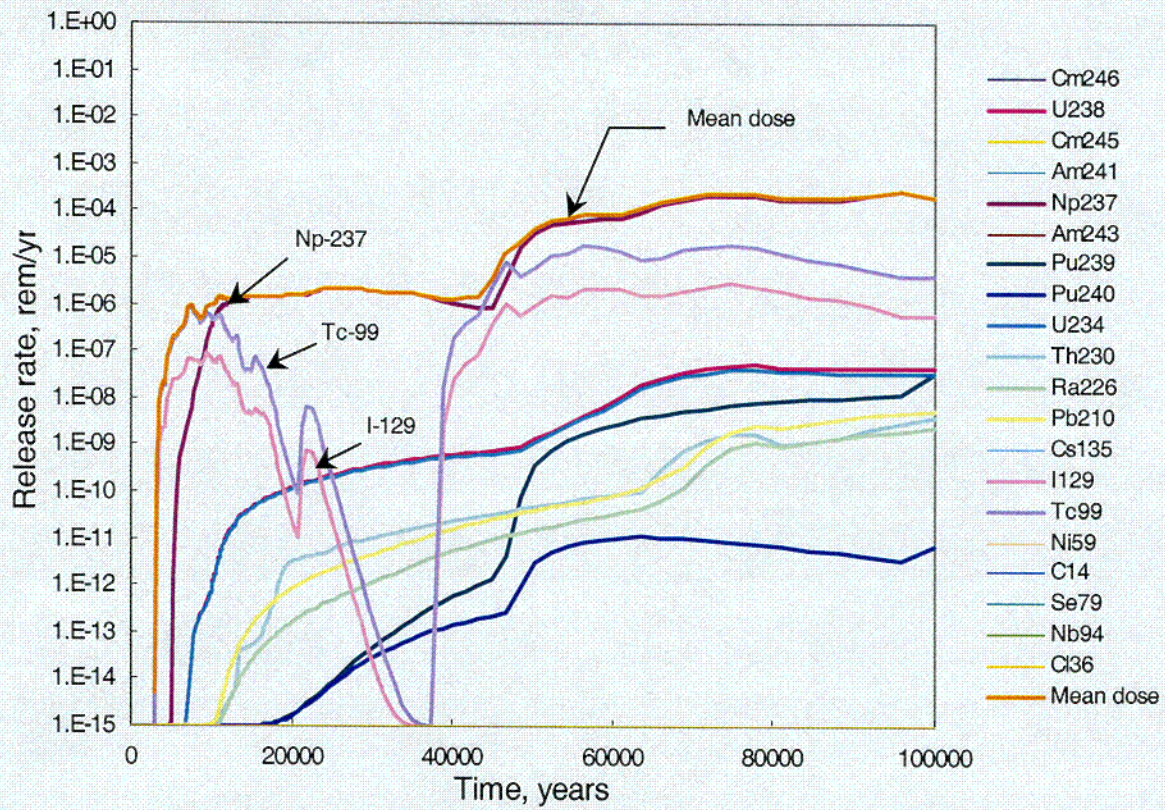


Fig. 11. Calculated release rates for various radionuclides for Case A from 200 realizations. The Case A that accounts for 4,667 metric tons of heavy metal of high-level waste glass refers to the parameters in Table 6.

CO2

## Figure captions

Fig. 1. Cumulative normalized leach concentration for boron versus time for WVDP Ref. 6 and DWPF Blend 1 glasses in various solutions at 90 °C

Fig. 2. Normalized leach rate for boron versus time for WVDP Ref. 6 and DWPF Blend 1 glasses in various solutions at 90 °C

Fig. 3. Normalized leach rates for various elements as a function of time for WVDP Ref. 6 glass in 0.25 M FeCl<sub>3</sub> solution at 90 °C

Fig. 4. Leachate pH versus time for WVDP Ref. 6 glass in various solutions at 90 °C (Closed symbols for the initial pH and open symbols for the final pH)

Fig. 5. Scanning electron micrographs of WVDP Ref. 6 glass (a) before leaching and after leaching in (b) deionized water and (c) 0.25 M FeCl<sub>3</sub> solution at 90 °C

Fig. 6. Normalized leach rate for various elements versus leachate pH after first solution replacement for (a) WVDP Ref. 6 and (b) DWPF Blend 1 glasses at various temperatures

Fig. 7. Linear regression of normalized leach rate for boron versus leachate pH after first solution replacement for (a) WVDP Ref. 6 and (b) DWPF Blend 1 glasses at various temperatures

Fig. 8. Comparison of calculated glass dissolution rates using different rate expressions

Fig. 9. Calculated mean dose rates for three cases from 200 realizations. The Cases A and B that account for 4,667 metric tons of heavy metal of high-level waste glass refer to the parameters in Table 6. The nominal case of the Total-system Performance Assessment code models 70,040 metric tons of heavy metal of spent nuclear fuel in the repository system.

Fig. 10. Calculated release rates for various radionuclides for the nominal case from 200 realizations. The nominal case of the Total-system Performance Assessment code models 70,040 metric tons of heavy metal of spent nuclear fuel in the repository system.

Fig. 11. Calculated release rates for various radionuclides for Case A from 200 realizations. The Case A that accounts for 4,667 metric tons of heavy metal of high-level waste glass refers to the parameters in Table 6.